PSFC/JA-10-65

Operation of a Continuously Frequency-Tunable Second-Harmonic CW 330-GHz Gyrotron for Dynamic Nuclear Polarization

Torrezan, A.C., Shapiro, M.A., Sirigiri, J.R.,
Temkin, R.J., Griffin, R.G.*

* Department of Chemistry and the Francis Bitter Magnet Laboratory,
Massachusetts Institute of Technology, Cambridge, MA 02139

2010

**Plasma Science and Fusion Center
Massachusetts Institute of Technology
Cambridge MA 02139 USA**

Operation of a Continuously Frequency-Tunable Second-Harmonic CW 330-GHz Gyrotron for Dynamic Nuclear Polarization

Antonio C. Torrezan, *Member, IEEE*, Michael A. Shapiro, Jagadishwar R. Sirigiri, *Member, IEEE*, Richard J. Temkin, *Fellow, IEEE,* and Robert G. Griffin

Abstract— The design and operation of a frequency tunable continuous-wave (CW) 330-GHz gyrotron oscillator operating at the second harmonic of the electron cyclotron frequency are reported. The gyrotron has generated 18 W of power from a 10.1-kV 190-mA electron beam working in a $TE_{-4,3}$ cylindrical mode, corresponding to an efficiency of 0.9%. The measured start oscillation current over a range of magnetic field values is in good agreement with theoretical start currents obtained from linear theory for successive high order axial modes $TE_{-4,3,q}$, where $q = 1$ to 6. Also, the observed frequency range in the start current measurement is in reasonable agreement with the frequency range calculated from numerical simulations. The minimum start oscillation current of the device was measured to be 33 mA. A continuous tuning range of 1.2 GHz was observed experimentally via a combination of magnetic, voltage, and thermal tuning. The gyrotron output power and frequency stabilities were assessed to be ±0.4% and ±3 ppm, respectively, during a 110-hour uninterrupted CW run. Evaluation of the gyrotron microwave output beam pattern using a pyroelectric camera indicated a Gaussian-like mode content of 92% with an ellipticity of 28%. The gyrotron will be used for 500-MHz nuclear magnetic resonance (NMR) experiments with sensitivity enhanced by dynamic nuclear polarization (DNP).

Index Terms—Dynamic nuclear polarization (DNP), nuclear magnetic resonance (NMR), second cyclotron harmonic, submillimeter wave, terahertz, tunable gyrotron.

I. INTRODUCTION

GYROTRON oscillators are vacuum electron devices that have delivered MW power levels at millimeter wavelengths [1], and kW power levels in the THz or submillimeter band [2], [3]. The lack of other sources able to match these power levels in the abovementioned bands, with the exception of much bulkier free electron lasers, makes the gyrotron the oscillator of choice in many applications such as plasma heating [1], materials processing [4], diagnostics [5], spectroscopy [6], and in non-lethal weapons [7]. Although the main attractiveness of the gyrotron resides in its power, some applications would also benefit from having a frequency tunable generator. For instance the operation of a nuclear magnetic resonance (NMR) spectrometer enhanced by dynamic nuclear polarization (DNP) would be greatly simplified by utilizing a continuously tunable continuous-wave (CW) gyrotron [8].

For efficient interaction between electrons and electromagnetic waves, gyrotron oscillators employ resonant structures with high quality factor, on the order of or greater than one thousand depending on the operating frequency. This limits the attainable frequency tunability of a given gyrotron cavity mode to the linewidth associated with its quality factor [9]. Another option for broader tunability is to excite successive cavity modes with eigenfrequencies close to each other by changing the electron cyclotron frequency by means of the gyrotron main magnetic field and/or the electron beam energy. As in gyrotron resonators the axial wavenumber is typically much smaller than the transverse wavenumber, cavity modes that only differ by their number of axial variations on their electric field profile may lead to continuous tunability. This tuning scheme was demonstrated in a millimeter-wave gyrotron operating in the first harmonic of the electron cyclotron frequency, both in pulsed mode [10] and continuous-wave mode [11], and later in a second-harmonic continuous-wave THz gyrotron [12], [13]. The smooth tuning range obtained in these experiments was equal to or greater than 1 GHz. Following these results, other gyrotrons using a similar magnetic tuning scheme have been built as described in [14], [15].

In this article, we report the design and operation of a second-harmonic continuous-wave 330-GHz gyrotron oscillator. Based on previous second-harmonic broadband magnetic and voltage tuning results at 332 GHz [12], [16], this tuning scheme was favored for the 330-GHz gyrotron instead of a more involved approach based on mechanical tuning [17], [18]. Besides further exploring the chosen tuning scheme, the 330-GHz gyrotron also features additional tuning by thermally expanding the resonator. The 330-GHz gyrotron is intended to be used as a THz source for a 500-MHz DNP/NMR spectrometer. This paper is organized as follows: the design of the gyrotron is described in Section II while Section III details the experimental characterization of the device including evaluation of output power and frequency as a function of magnetic field, beam voltage, and cavity cooling temperature. Measured start oscillation current of the operating mode, frequency and power stability in long-run continuous operation, and output microwave beam profile are also reported in Section III. Conclusions follow in Section IV.

II. DESIGN

The 330-GHz gyrotron oscillator is shown schematically in Fig. 1. This gyrotron employs a diode magnetron injection gun described in [13]. The electron gun is connected to a CW power supply able to provide a maximum voltage of 25 kV and a maximum current of 200 mA, restricted to a maximum total power of 4 kW. The beam tunnel section between the electron gun and the gyrotron resonator is composed of a series of slotted tubes and a piece of lossy SiC ceramic to prevent spurious oscillations before the interaction region. The electron beam radius at the oscillator beam-wave interaction section is $r_e = 1.08$ mm. The high coupling coefficient of the second-harmonic cylindrical mode TE$_{-4,3}$ at this beam radius along with previous experiments carried out in this mode at 332 GHz [12], [16], motivated its choice as the gyrotron operating mode. The profile of the designed oscillator interaction circuit is presented in Fig. 2, where the inset shows the position of the electron beam with respect to the transverse electric field profile of the operating cavity mode TE$_{-4,3}$. A long interaction cavity straight section was preferred in order to lower the start oscillation current and facilitate the excitation of high-order axial modes TE$_{-4,3,q}$ for frequency tunability via magnetic and voltage tuning. The indices m, p, and q associated with a cylindrical mode TE$_{m,p,q}$ correspond to the azimuthal, radial, and axial mode numbers, respectively.

The ohmic quality factor Q_O for the different axial modes TE$_{-4,3,q}$ was calculated to be $Q_O = 10150$ assuming an electrical conductivity half that of ideal copper (5.8×10^7 S/m). The eigenfrequency and diffraction quality factor $Q_{D,q}$ of each axial mode were computed using a cold-cavity code [19] and the results are presented in Table I.

TABLE I
COLD-CAVITY PARAMETERS FOR TE$_{-4,3,q}$ MODES

q	Cold resonant frequency [GHz]	Q_D
1	329.96	81500
2	330.03	20400
3	330.15	9050
4	330.32	5080
5	330.54	3230
6	330.81	2230
7	331.13	1670

From the calculated quality factors and the cold axial electric field profile, the start oscillation current for the operating and neighboring modes were computed using linear theory [20]. The start current for the first axial variation ($q = 1$) of each mode is shown in Fig. 3(a) for beam parameters beam voltage $V_b = 10.1$ kV, pitch factor $\alpha = 1.8$, $r_e = 1.08$ mm, and no velocity spread. The minimum start current for the mode TE$_{-4,3,1}$ was computed to be 31 mA. The calculated start current for the high-order axial operating modes TE$_{-4,3,q}$ and the adjacent mode, the fundamental-harmonic mode TE$_{5,1,1}$, are displayed in Fig. 3(b) for the same beam parameters. Based on the start current calculation and the current limit of 200 mA in the available power supply, linear theory predicts that it may be possible to excite high-order axial modes that would yield a tuning range on the order of 1 GHz in this gyrotron.

The gyrotron interaction circuit was electroformed from oxygen-free copper using a stainless steel mandrel machined to a tolerance of 2.5 μm in cavity diameter and with a surface finish of 0.2 μm. The fabricated cavity was cold tested following the procedure outlined in [13], and the cavity radius was estimated to be $r_{cav} = 1.834$ mm, which is within manufacturing tolerance.

After the beam-wave interaction, the generated wave is extracted from the gyrotron oscillator by converting the cylindrical operating mode to a Gaussian-like microwave beam. The mode converter consists of a helical launcher with waveguide radius $r_{wg} = 2.85$ mm, a quasi-parabolic smooth mirror, and two additional smooth mirrors. The mode converter design was evaluated using the electric field integral equation code Surf3d [21]. The results from these calculations are shown in Fig. 4, where the Gaussian-like content of the output beam at the focal plane was computed to be 92% with beam radii $w_x = 3.3$ mm and $w_y = 4.2$ mm.

III. EXPERIMENTAL RESULTS

The 330-GHz second-harmonic gyrotron was characterized in CW mode with a 19-mm diameter corrugated waveguide connected to the gyrotron output. The output power of the oscillator was measured using a Scientech laser disc calorimeter, model 36-0401, whereas the frequency was measured using a heterodyne system detailed in [13]. Table II summarizes the main operating parameters of the 330-GHz gyrotron oscillator.

TABLE II
GYROTRON OPERATING PARAMETERS

Operating mode $TE_{m,p,q}$	$TE_{-4,3,q}$
Frequency	328.8 – 330 GHz
Frequency tuning range	1.2 GHz
Output power	2 – 18 W (CW)
Cavity magnetic field B_0	6.0 T
Cyclotron harmonic	Second
Beam voltage V_b	< 13 kV
Beam current I_b	190 mA

A. Start Oscillation Current

The start oscillation current of the operating mode $TE_{-4,3}$ was evaluated as a function of the magnetic field B_0 for a fixed beam voltage $V_b = 10.1$ kV. The measured start current as well as the measured frequency at each start current value are displayed in Fig. 5 by a solid line and by diamonds, respectively. The minimum start current was measured to be 33 mA. Also plotted in Fig. 5 are the theoretical start currents for the first six axial modes $TE_{-4,3,q}$, where $q = 1$ to 6. The theoretical start currents were obtained from linear theory for beam parameters $V_b = 10.1$ kV, $\alpha = 1.8$, and no velocity spread. The start current calculations assumed a cavity radius $r_{cav} = 1.833$ mm for best fit, which is within the experimental error of the value (1.834 mm) obtained from the cavity cold test, as well as the axial electric field profile obtained from the cold-cavity code.

Good agreement is obtained between the measured start current and the prediction from linear theory, suggesting that high-order axial modes are being observed in the experiment. In addition, the measured frequency range for the start current between 329.88 GHz and 331.13 GHz is in reasonable agreement with the range for high-order axial modes presented in Table I. Frequency detuning may exist at the lower edge of the excitation zone for $B_0 < 6.01$ T since the measured power at these start current values is greater than 1.4 W. The neighboring fundamental mode $TE_{5,1}$ is excited for magnetic field values $B_0 > 6.035$ T.

B. Power and Frequency Tuning

The 330-GHz gyrotron has generated 18 W of output power in the second-harmonic mode $TE_{-4,3}$ for a 10.1-kV 190-mA electron beam, which corresponds to an efficiency of 0.93%. A smooth continuous frequency tuning range of 1 GHz has been achieved as a function of magnetic field as shown in Fig. 6. In the magnetic tuning measurement, the gyrotron output power was optimized by adjusting the subtracting gun coil field from $B_{gun} = -3$ mT to $B_{gun} = -5$ mT as the main magnetic field was increased, resulting in a minimum output power of 2 W throughout the frequency tuning range.

Comparing the magnetic tuning data with the measured start current, one can verify that microwaves are being excited at current values lower than the start current for $B_0 < 6.0$ T. This region corresponds to the hard excitation region and it is accessible by lowering the magnetic field after first exciting microwaves at a higher magnetic field value. Another difference between Fig. 5 and Fig. 6 is a frequency downshift seen in the magnetic tuning measurement. This frequency shift is a result of cavity thermal expansion under higher average power operation and it was not observed in pulsed mode operation with a duty cycle of 0.004%.

Due to the dependence of the electron cyclotron frequency on beam voltage, a continuous tuning range of 1 GHz was also achieved as a function of beam voltage for a constant magnetic field as indicated in Fig. 7. As the beam voltage was decreased from the maximum power point, the gun coil field had to be adjusted from $B_{gun} = 1$ mT to $B_{gun} = -25$ mT to optimize the gyrotron power for a beam current $I_b = 190$ mA.

The power and tuning response obtained using voltage tuning are similar to the ones measured for magnetic tuning as shown in Fig. 8 by plotting the voltage and magnetic tuning results as a function of the normalized electron cyclotron frequency. One advantage of voltage tuning over magnetic tuning is the possibility to sweep the gyrotron frequency at a faster rate, which may be explored for instance in future DNP/NMR experiments.

Another feature evaluated in the 330-GHz gyrotron was frequency tunability via thermal tuning. By increasing the water temperature T_{water} in the cavity cooling channel via a commercial chiller/heater system, the gyrotron cavity will expand and the beam voltage necessary to keep the same synchronism and efficiency condition has to be increased for a fixed magnetic field. This effect is observed in the measurement shown in Fig. 9 as the power curve shifts to higher voltage values as the water temperature is increased from 11°C to 57°C. An additional tuning range of 250 MHz was obtained using thermal tuning.

C. CW Long-Term Stable Operation

Stable gyrotron operation over extended periods without interruption is an important requirement to allow long-term signal averaging in DNP/NMR experiments. The stability of the 330-GHz gyrotron was evaluated during a 110-h continuous run test and the result is shown in Fig. 10. In this test, the output power was kept stable using a proportional, integral, and derivative (PID) computerized control system by adjusting the cathode filament current based on the difference between a set point value and the measured output power. The output power was sampled using a Scientech calorimeter head, model AC2500. During the

stability test, the output reference power and frequency were kept stable within ±0.4% (±3 mW) and ±3 ppm (±1.1 MHz), respectively, meeting the requirement for DNP/NMR.

D. Output Beam Pattern

The output microwave beam pattern of the 330-GHz gyrotron was quantitatively evaluated based on measurements taken at the corrugated waveguide output using a Spiricon Pyrocam III pyroelectric camera. Due to the camera maximum power limit of 2 W, a picture of the output beam was taken at low power (0.4 W) and it is shown in Fig. 11. The Gaussian-like content associated with the measured pattern was calculated to be 92% with beam waists w_x = 5.1 mm and w_y = 4.0 mm, indicating a suitable operation of the fabricated mode converter.

IV. CONCLUSION

The second-harmonic 330-GHz gyrotron oscillator has generated 18 W of power from a 10.1-kV 190-mA electron beam working in a $TE_{-4,3}$ cylindrical mode, which corresponds to an efficiency of 0.93%. Good agreement is obtained between the measured start oscillation current and the theoretical start currents calculated from linear theory for successive high order axial modes $TE_{-4,3,q}$, where q = 1 to 6. In addition, the observed frequency range in the start current measurement is in reasonable agreement with the frequency range expected from numerical calculations. The minimum start oscillation current of the oscillator was measured to be 33 mA. A continuous frequency tuning range of 1.0 GHz with minimum output power of 2 W was experimentally achieved via magnetic and voltage tuning. While the results from these two tuning schemes basically overlapped, voltage tuning presents as an option to tune the gyrotron frequency at a faster rate, a feature that may be explored by some applications such as DNP/NMR. Thermal tuning was also implemented and assessed in this tube, yielding an additional tuning range of 250 MHz. Another aspect of the source relevant for the 500-MHz DNP/NMR application for which the gyrotron was designed is frequency and power stability. The gyrotron output power and frequency stabilities were measured to be ±0.4% and ±3 ppm, respectively, during a 110-hour uninterrupted CW run. The gyrotron microwave output beam pattern was also measured using a pyroelectric camera and it has a Gaussian-like mode content of 92% with an ellipticity of 28%, indicating a suitable operation of the manufactured mode converter.

REFERENCES

[1] M. K. A. Thumm, "Recent developments on high-power gyrotrons - introduction to this special issue," *J. Infrared Milli. Terahz Waves*, DOI: 10.1007/s10762-010-9754-5, 2010.

[2] V. L. Bratman, M. Yu. Glyavin, Yu. K. Kalynov, A. G. Litvak, A. G. Luchinin, A. V. Savilov, and V. E. Zapevalov, "Terahertz gyrotrons at IAP RAS: status and new designs," *J. Infrared Milli. Terahz Waves*, DOI: 10.1007/s10762-010-9689-x, 2010.

[3] S. Spira-Hakkarainen, K. E. Kreischer, and R. J. Temkin, "Submillimeter-wave harmonic gyrotron experiment," *IEEE Trans. Plasma Sci.*, vol. 18, no. 3, pp. 334–342, Jun. 1990.

[4] K. L. Felch, B. G. Danly, H. R. Jory, K. E. Kreischer, W. Lawson, B. Levush, and R. J. Temkin, Characteristics and applications of fast-wave gyrodevices," *Proc. IEEE*, vol. 87, no. 5, pp. 752-781, May 1999.

[5] H. Bindslev, J. A. Hoekzema, J. Egedal, J. A. Fessey, T. P. Hughes, and J. S. Machuzak, "Fast-ion velocity distributions in JET measured by collective Thomson scattering," *Phys. Rev. Lett.*, vol. 83, no. 16, pp. 3206-3209, Oct. 1999.

[6] L. R. Becerra, G. J. Gerfen, R. J. Temkin, D. J. Singel, and R. G. Griffin, "Dynamic nuclear polarization with a cyclotron resonance maser at 5 T," *Phys. Rev. Lett.*, vol. 71, no. 21, pp. 3561-3564, Nov. 1993.

[7] K. Felch, M. Blank, P. Borchard, P. Cahalan, S. Cauffman and H. Jory, "Recent test results on a 95 GHz, 2 MW gyrotron," in *Proc. 33rd Int. Conf. on Infrared, Millimeter and THz Waves*, Pasadena, CA, Sep. 2008, pp. 1-2.

[8] V. S. Bajaj, M. K. Hornstein, K. E. Kreischer, J. R. Sirigiri, P. P. Woskov, M. L. Mak-Jurkauskas, J. Herzfeld, R. J. Temkin, and R. G. Griffin, "250 GHz CW gyrotron oscillator for dynamic nuclear polarization in biological solid state NMR," *J. Magn. Reson.*, vol. 189, pp. 251-279, 2007.

[9] Y. V. Zasypkin, "Electronic frequency tuning in gyrotrons," *Sov. J. Commun. Technol. Electron.*, vol. 33, no. 5, pp. 7-13, May 1988.

[10] M. K. Hornstein, V. S. Bajaj, R. G. Griffin, K. E. Kreischer, I. Mastovsky, M. A. Shapiro, J. R. Sirigiri, and R. J. Temkin, "Second harmonic operation at 460 GHz and broadband continuous frequency tuning of a gyrotron oscillator," *IEEE Trans. Electron Devices*, vol. 52, no. 5, pp. 798-807, May 2005.

[11] M. K. Hornstein, V. S. Bajaj, R. G. Griffin, and R. J. Temkin, "Efficient low-voltage operation of a CW gyrotron oscillator at 233 GHz," *IEEE Trans. Plasma Sci.*, vol. 35, no. 1, pp. 27-30, Feb. 2007.

[12] A. C. Torrezan, S.-T. Han, M. A. Shapiro, J. R. Sirigiri, and R. J. Temkin, "CW operation of a tunable 330/460 GHz gyrotron for enhanced nuclear magnetic resonance," in *Proc. 33rd Int. Conf. on Infrared, Millimeter and THz Waves*, Pasadena, CA, Sep. 2008, pp. 1-2.

[13] A. C. Torrezan, S.-T. Han, I. Mastovsky, M. A. Shapiro, J. R. Sirigiri, R. J. Temkin, A. B. Barnes, and R. G. Griffin, "Continuous-wave operation of a frequency-tunable 460-GHz second-harmonic gyrotron for enhanced nuclear magnetic resonance," *IEEE Trans. Plasma Sci.*, vol. 38, no. 6, pp. 1150-1159, Jun. 2010.

[14] T. H. Chang, T. Idehara, I. Ogawa, L. Agusu, and S. Kobayashi, "Frequency tunable gyrotron using backward-wave components," *J. Appl. Phys.*, vol. 105, p. 063304, Mar. 2009.

[15] T. Idehara, K. Kosuga, L. Agusu, R. Ikeda, I. Ogawa, T. Saito, Y. Matsuki, K. Ueda, and T. Fujiwara, "Continuously frequency tunable high power sub-THz radiation source - Gyrotron FU CW VI for 600 MHz DNP-NMR spectroscopy," *J. Infrared Milli. Terahz Waves*, vol. 31, no. 7, pp. 775-790, Jul. 2010.

[16] A. C. Torrezan, M. A. Shapiro, J. R. Sirigiri, and R. J. Temkin, "A tunable continuous-wave 330 GHz gyrotron for enhanced nuclear magnetic resonance," in *Proc. IEEE 36th Int. Conf. Plasma Sci.*, San Diego, CA, Jun. 2009, p. 1.

[17] I. I. Antakov, S. N. Vlasov, V. A. Gintsburg, L. I. Zagryadskaya, and L. V. Nikolaev, "CRM-oscillators with mechanical tuning of frequency," *Elektron. Tekhn.*, Ser. I, Elektron. SVCh, no. 8, pp. 20–25, 1975.

[18] G. F. Brand, Z. Chen, N. G. Douglas, M. Gross, J. Y. L. Ma, and L. C. Robinson, "A tunable millimetre-submillimetre gyrotron," *Int. J. Electron.*, vol. 57, no. 6, pp. 863–870, 1984.

[19] A. W. Fliflet, and M. E. Read, "Use of weakly irregular waveguide theory to calculate eigenfrequencies, Q values, and RF field functions for gyrotron oscillators," *Int. J. Electron.*, vol. 51, no. 4, pp. 475-484, 1981.

[20] M. Yeddulla, G. S. Nusinovich, and T. M. Antonsen, Jr., "Start currents in an overmoded gyrotron," *Phys. Plasmas*, vol. 10, no. 11, pp. 4513-4520, Nov. 2003.

[21] J. M. Neilson, and R. Bunger, "Surface integral equation analysis of quasi-optical launcher," *IEEE Trans. Plasma Sci.*, vol. 30, no. 3, pp. 794-799, Jun. 2002.

Ion Pump

Ceramic Break

Water-cooled
Collector

Mode Converter   Window

Mirrors   Microwaves

Mo Beam Scraper   Water-cooled Cavity

Superconducting
Magnet
(± 8.0 T)

                                          SiC Ceramic

Beam Tunnel   Slotted Tubes

Gun Coil
(± 0.3 T)
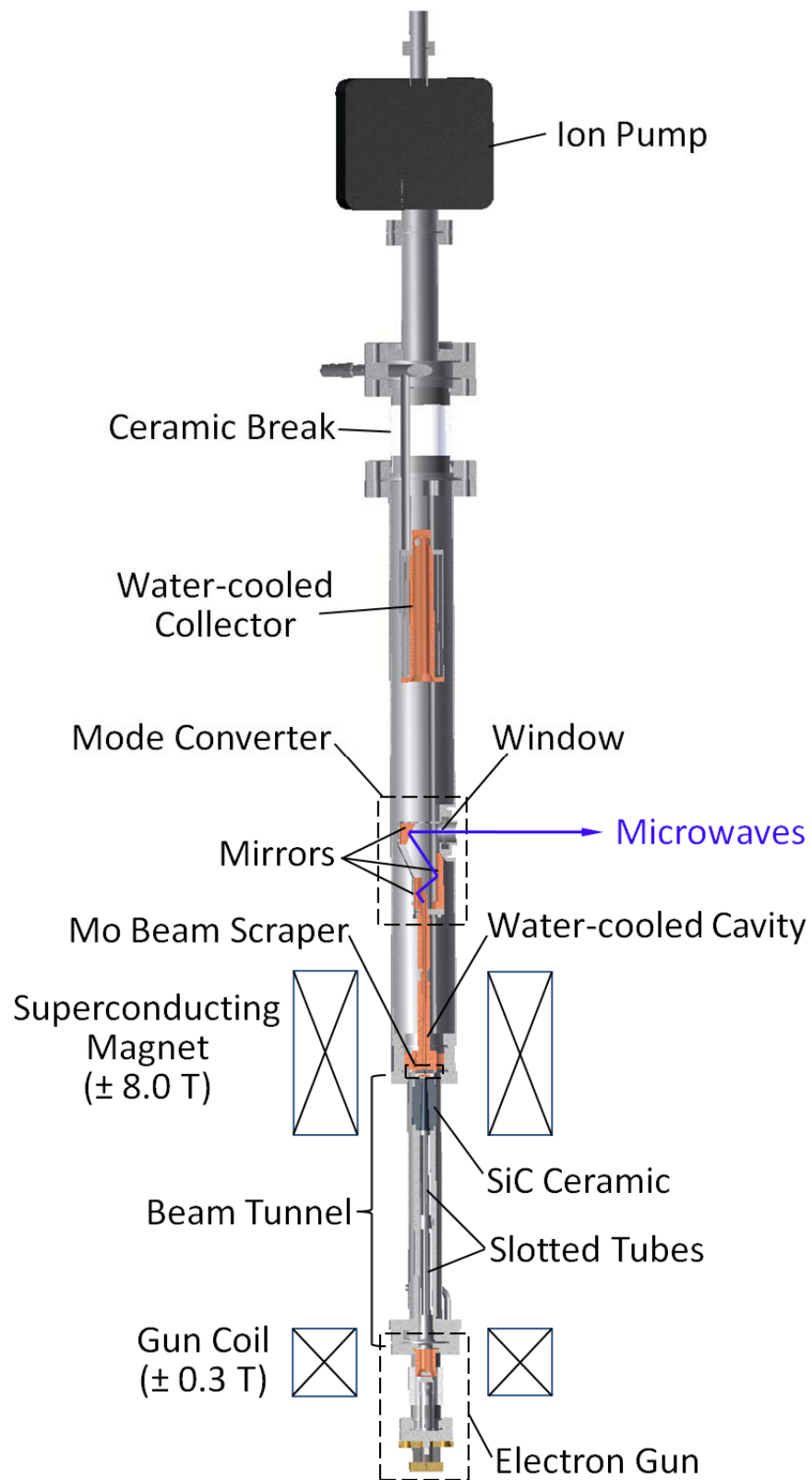
                                          Electron Gun

Fig. 1. Schematic of the 330-GHz gyrotron oscillator.
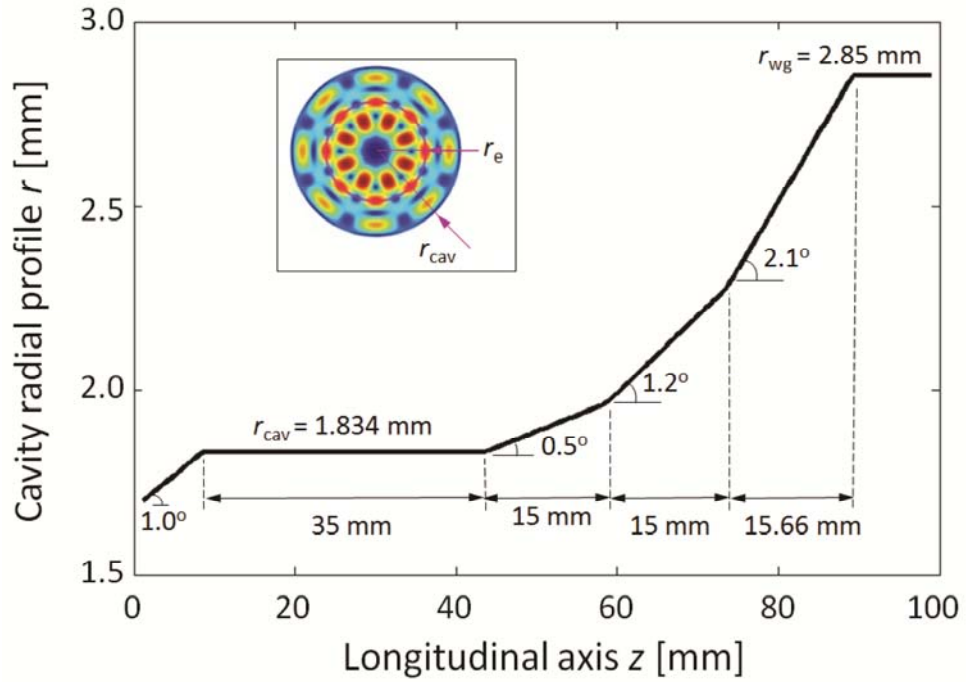
Fig. 2. Schematic of the 330-GHz gyrotron interaction circuit. The inset shows the transverse electric field profile of the cavity mode TE$_{-4,3}$ and the location of the electron beam with radius $r_e = 1.08$ mm.
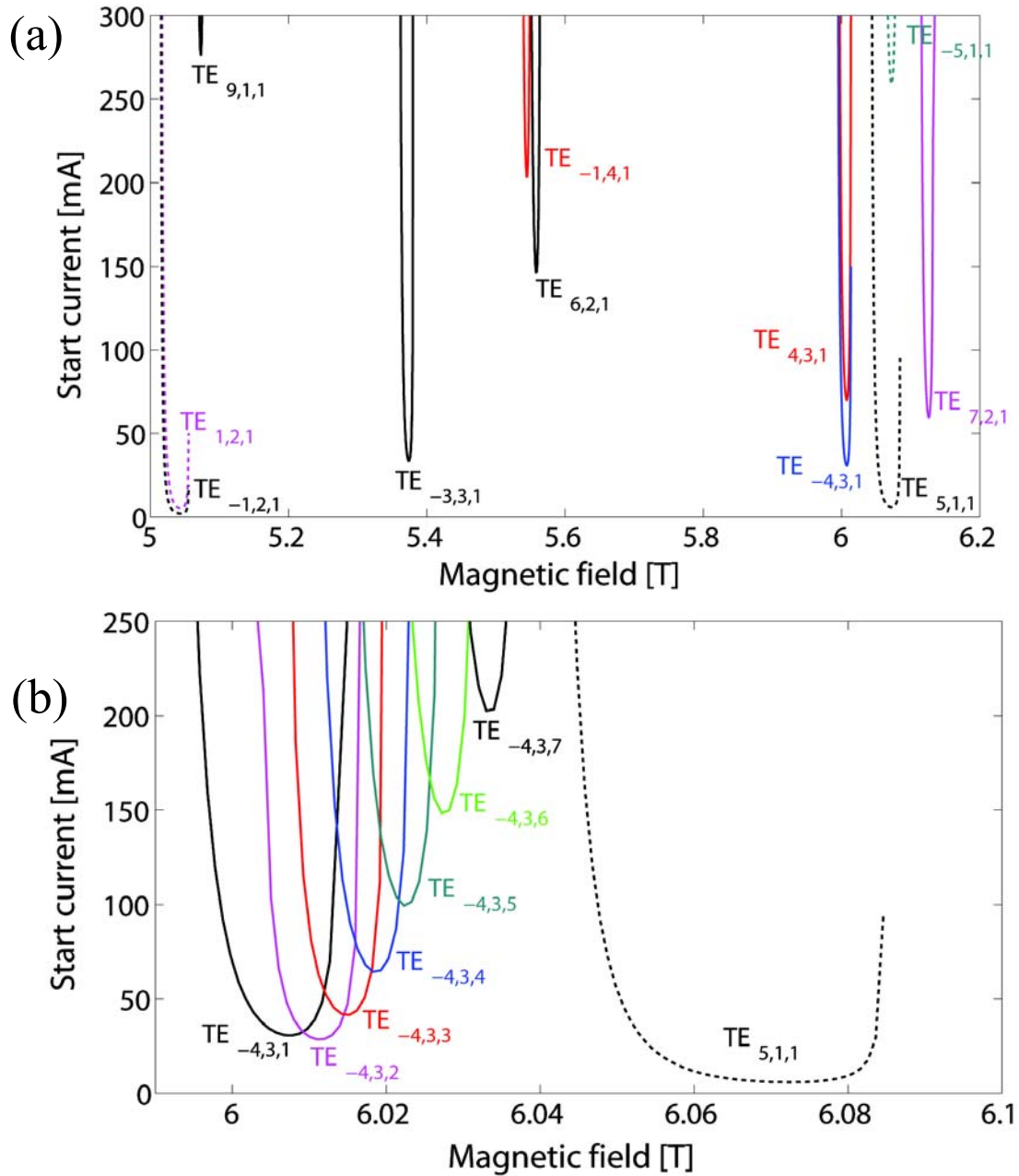
Fig. 3. (a) Calculated start oscillation current of cavity $TE_{m,p,1}$ modes adjacent to the operating mode $TE_{-4,3,1}$; (b) calculated start current of high-order axial operating modes $TE_{-4,3,q}$, where $q = 1$ to 7, and neighboring fundamental mode $TE_{-5,1,1}$. In (a) and (b) dashed lines represent fundamental-harmonic modes while solid lines refer to second-harmonic modes (Beam parameters: $V_b = 10.1$ kV, $r_e = 1.08$ mm, $\alpha = 1.8$, and no velocity spread).
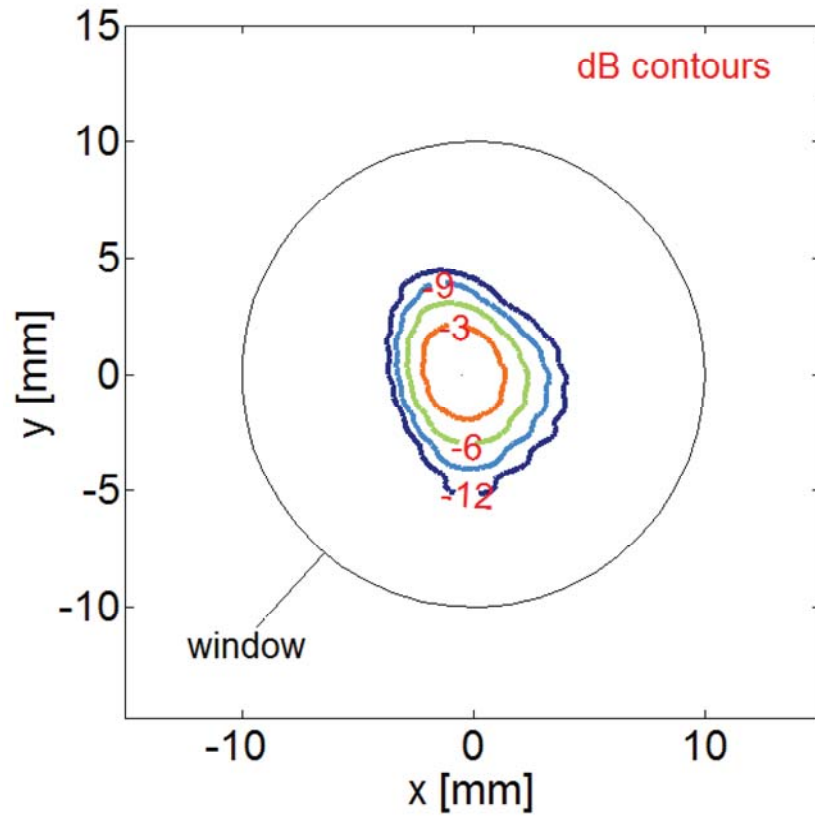
Fig. 4. Simulated electric field of 330-GHz microwave output beam at the focal plane. The gyrotron window is shown as a reference.
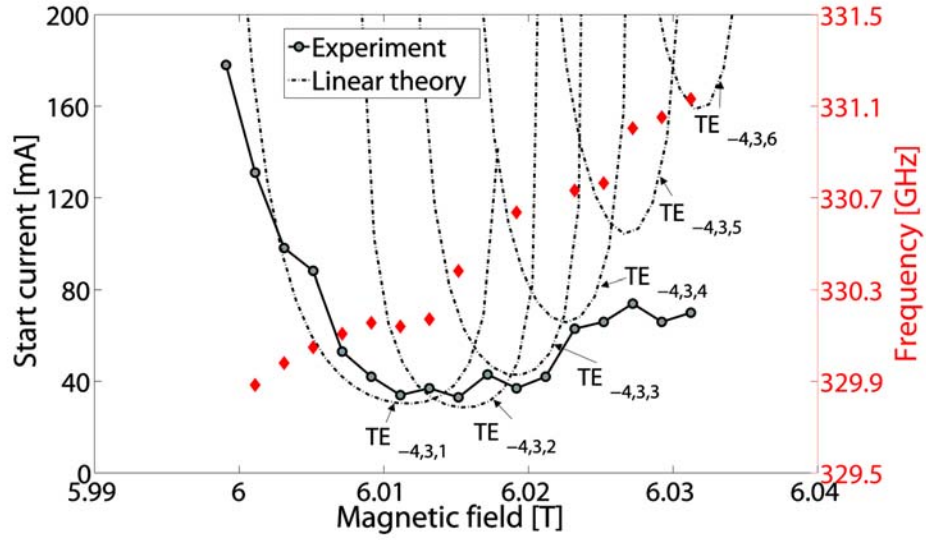
Fig. 5. Measured start oscillation current (solid line) and measured frequency (diamonds) of the operating mode TE$_{-4,3}$ as a function of magnetic field for beam voltage $V_b = 10.1$ kV, and water temperature in the cavity cooling channel $T_{water} = 20°C$. The theoretical start currents for the first six axial modes TE$_{-4,3,q}$, where $q = 1, 2, 3, 4, 5, 6$, are shown as dash-dotted lines and they were computed using linear theory (simulation parameters: $r_{cav} = 1.833$ mm, cold-cavity axial field profile, $V_b = 10.1$ kV, $\alpha = 1.8$, and no beam velocity spread).
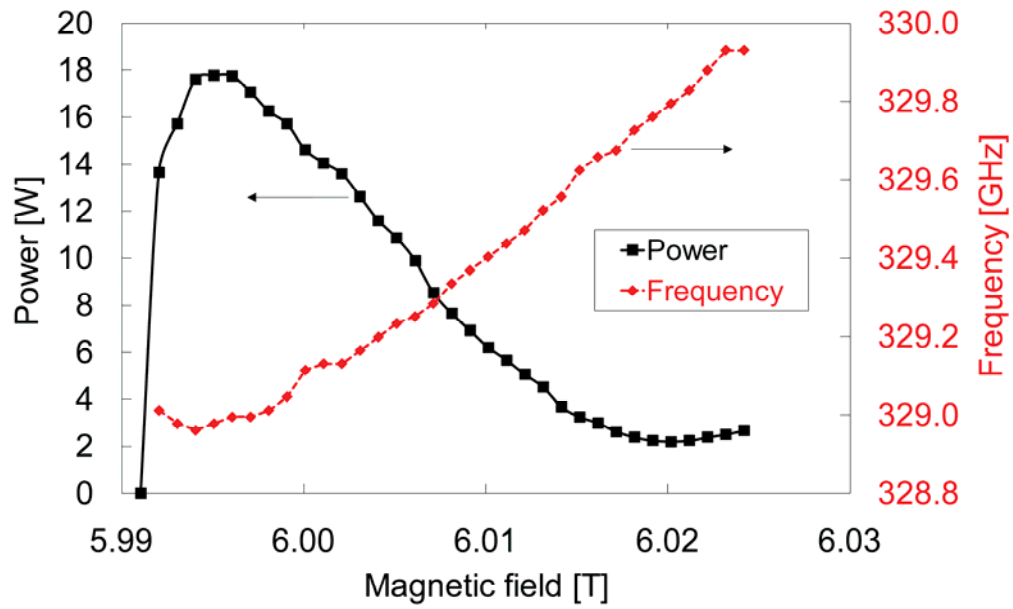
Fig. 6. Power (solid line) and frequency tuning (dashed line) measurement as a function of magnetic field for beam voltage V_b = 10.1 kV, beam current I_b = 190 mA, and cavity cooling channel temperature T_{water} = 9°C. The gun coil was swept from B_{gun} = −3 mT to B_{gun} = −5 mT for best output power as the magnetic field was increased.

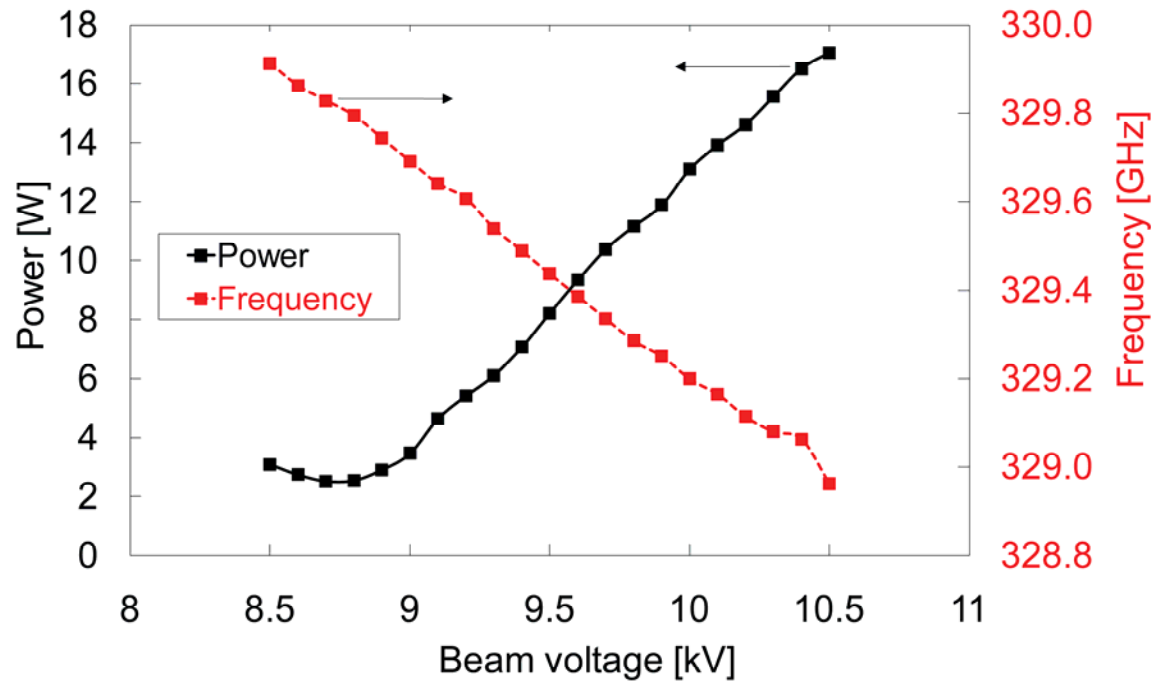Fig. 7. Power (solid line) and frequency tuning (dashed line) measurement as a function of beam voltage for magnetic field $B_0 = 6.003$ T, beam current $I_b = 190$ mA and cavity cooling channel temperature $T_{water} = 9°C$. The gun coil was swept from $B_{gun} = 1$ mT to $B_{gun} = -25$ mT for best output power as the beam voltage was decreased.
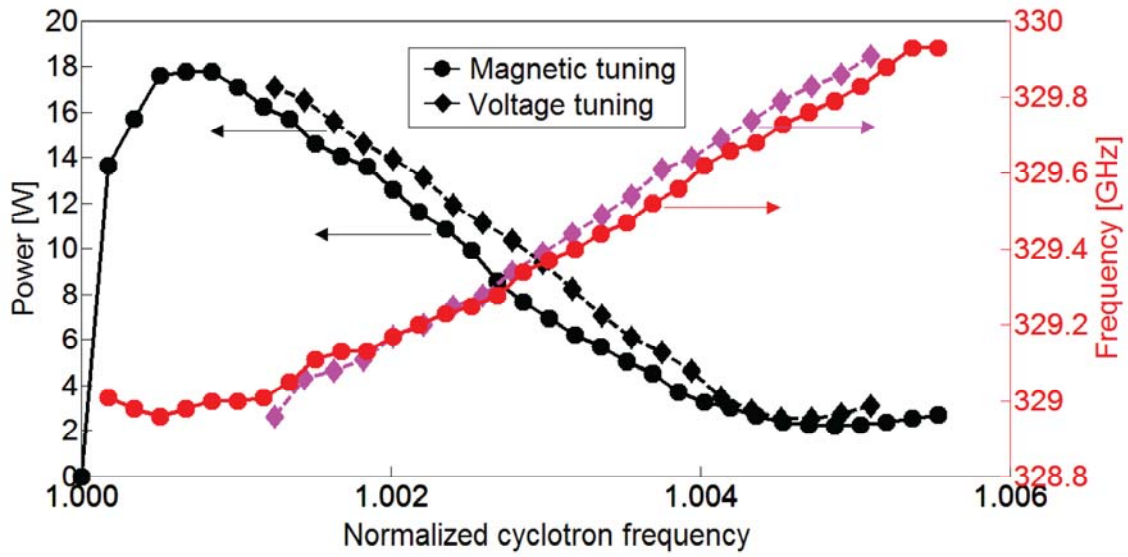
Fig. 8. Magnetic tuning (circular marks) and voltage tuning (diamond marks) measurement for beam current I_b = 190 mA, and cavity cooling channel temperature T_{water} = 9°C. The magnetic and voltage tuning data were taken at V_b = 10.1 kV and B_0 = 6.003 T, respectively.
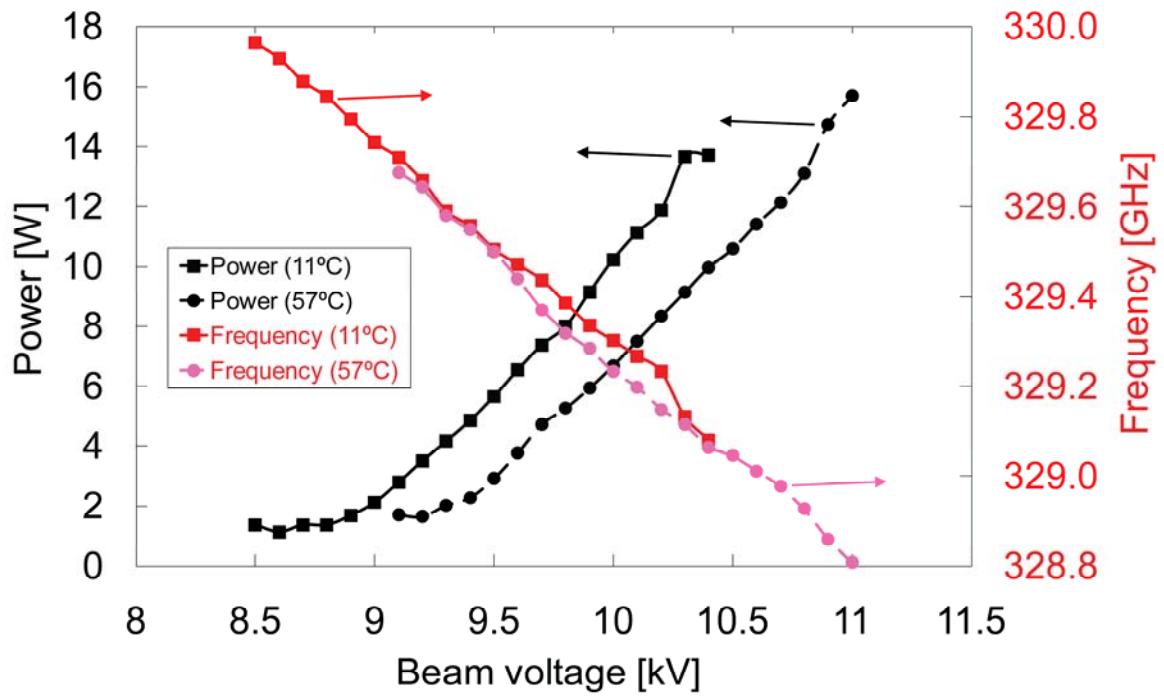
Fig. 9. Voltage tuning measurement for magnetic field $B_0 = 6.003$ T, beam current $I_b = 150$ mA, as well as cavity cooling channel temperature $T_{water} = 11°C$ (square markers), and $T_{water} = 57°C$ (circular markers).
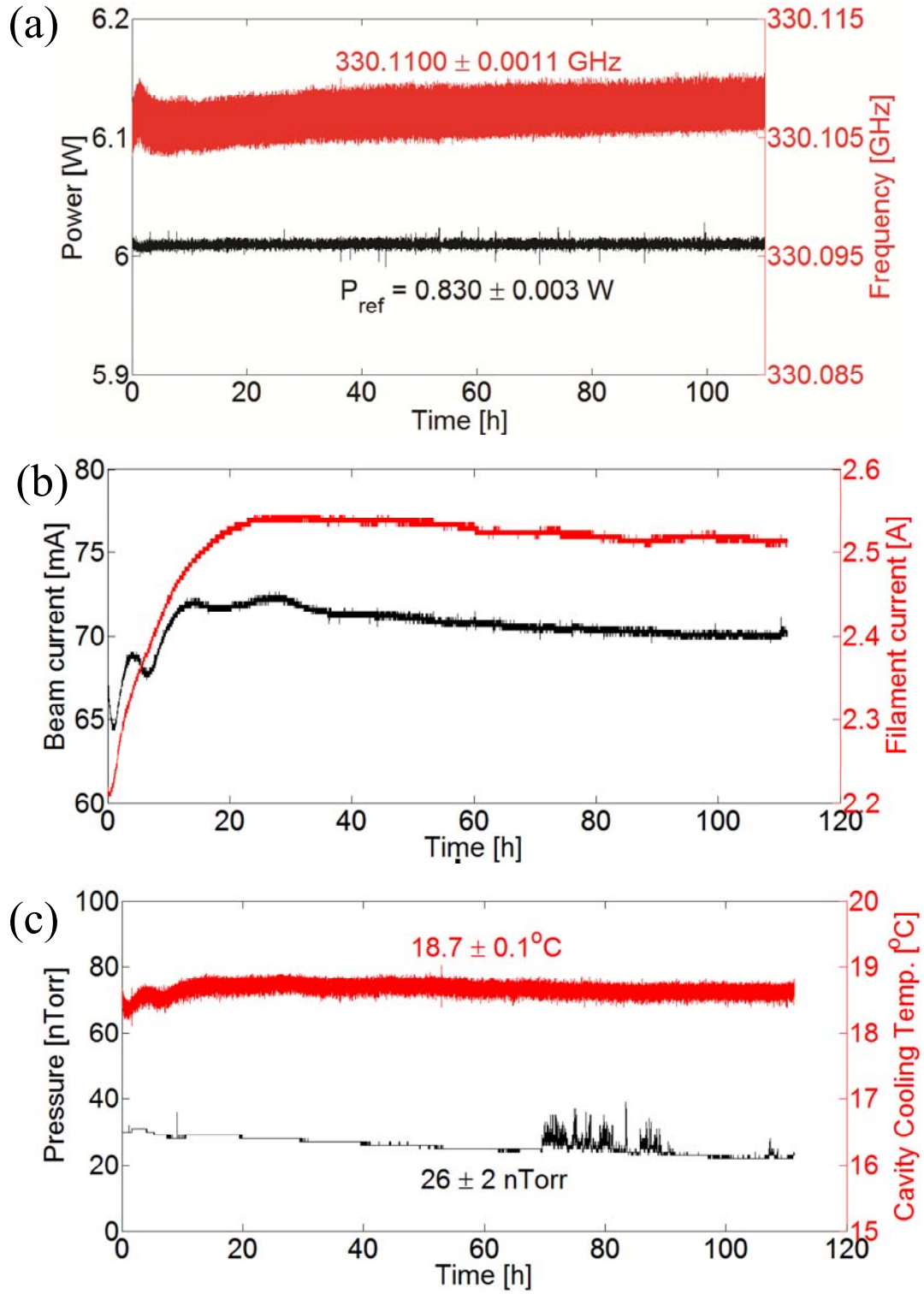
Fig. 10. Monitored variables during the CW long-run stability test of the 330-GHz second-harmonic gyrotron: (a) output power and frequency, (b) beam and cathode filament currents, and (c) pressure and cavity cooling temperature. During the test, the magnetic field was persistent at $B_0 = 6.006$ T and the beam voltage was fixed at $V_b = 10.0$ kV.
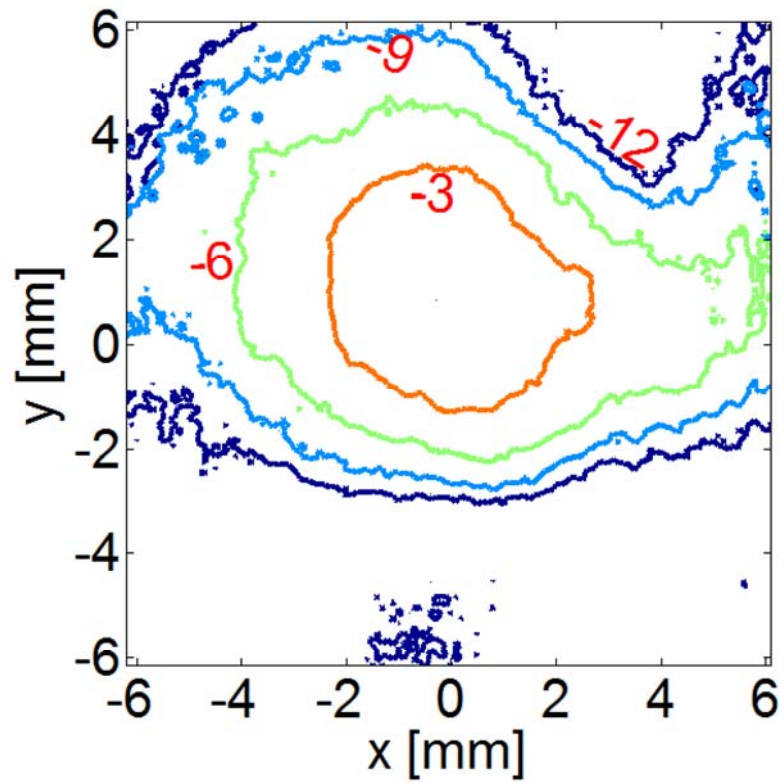
Fig. 11. Gyrotron output microwave beam pattern captured by a pyroelectric camera after the end of the corrugated waveguide. The beam pattern is displayed in dB contours. Gyrotron parameters: magnetic field B_0 = 6.003 T, beam voltage V_b = 9.6 kV, beam current I_b = 32 mA, frequency = 330.17 GHz, and output power of 0.4 W.